Spin Multiplicity Effects on the Second Hyperpolarizability of an Open-Shell Neutral π-Conjugated System

Masayoshi Nakano,*,†,‡ Tomoshige Nitta,† Kizashi Yamaguchi,§ Benoît Champagne,‡ and Edith Botek‡

Division of Chemical Engineering, Department of Materials Engineering Science, Graduate School of Engineering Science, Osaka University, Toyonaka, Osaka 560-8531, Japan, Laboratoire de Chimie Théorique Appliquée Facultés, Universitaires Notre-Dame de la Paix, rue de Bruxelles, 61, 5000 Namur, Belgium, and Department of Chemistry, Graduate School of Science, Osaka University, Toyonaka, Osaka 560-0043, Japan

Received: January 26, 2004; In Final Form: March 13, 2004

The spin multiplicity effects on the second hyperpolarizability (γ) are investigated for a small-size open-shell neutral conjugated model, the C_5H_7 radical, in the doublet, quartet, and sextet states by using several ab initio molecular orbital and density functional theory methods. The spatial contributions of total, α- and β-electrons to γ are examined to characterize the spin polarization and electron correlation effects on γ. It turns out that the second hyperpolarizability increases with the spin multiplicity, suggesting the interest of designing spin-enhanced nonlinear optical (NLO) systems based on open-shell neutral organic compounds, which also present the possibility of spin control of the NLO properties.

1. Introdunction

The quest for highly efficient nonlinear optical organic systems during the last three decades has mostly focused on closed-shell conjugated compounds.[1−10] Key strategies involve the optimization of the nature and length of the conjugated linker and the choice of donor and acceptor substituents of specific strengths, as well as the investigation of the effects of charging the system.[11−23] Although several studies have highlighted their potential,[14,17,24−30] much less has been achieved for open-shell systems for which the spin state constitutes another degree of freedom that could be tuned to match the desired properties or to be used in logic devices.

Open-shell systems can be classified according to the strength of electron correlation, i.e., weak, intermediate, and strong (magnetic) correlation regimes, which can be exemplified by equilibrium, intermediate, and long bond distance regions of a homogeneous neutral diatomic molecule.[31] Previous studies by three of us[32,33] indicate the remarkable variation in second hyperpolarizability (γ) according to increasing the bond distance and suggest the enhancement of γ in the intermediate correlation regime. In addition, the amplitude of the electron correlation is expected to change by modulating the spin and/or the charge of a system. In this study, as a first step toward realizing spin-modulated NLO systems, we focus on the dependency of γ on the spin state (doublet, quartet, and sextet). Namely, we investigate the static longitudinal second hyperpolarizabilities of the small-size neutral π-conjugated model, the C_5H_7 radical. Since significant electron correlation dependency and spin contamination effects are predicted for γ of such open-shell system,[26−28] we employ the UHF and *post*-UHF methods as well as spin-projected methods. In addition to γ values, the spatial contributions of total, α- and β-electrons to γ are characterized by using the hyperpolarizability density analysis[13,34] to investigate the spin polarization and electron correlation effects on γ. On the basis of the present results, the relationships among spin states and γ values for open-shell neutral systems are discussed in connection with the proposal of a new class of NLO systems, i.e. spin-enhanced NLO systems, which also present the possibility of spin control of NLO properties.

2. Methodology

2.1. Geometrical Structure. Figure 1 shows the structures of C_5H_7 radicals in the doublet (a), quartet (b), and sextet (c) states optimized at the UB3LYP level of approximation, using the 6-311G* basis set. The doublet, quartet, and sextet states are characterized by an excess of α-electrons with respect to β-electrons: one α-electron in excess for the doublet, three for the quartet, and five for the sextet. For each spin multiplicity the lowest energy state has been considered. At the B3LYP/6-311G* level, the corresponding $\langle S^2 \rangle$ values are 0.795, 3.765, and 8.765 for the doublet, quartet, and sextet whereas the exact values are 0.75, 3.75, and 8.75, respectively. The CC bond length alternation is shown to decrease when going from the doublet to the sextet state, where all CC bonds are similar to single bonds. This feature can be understood by the fact that increasing the spin multiplicity corresponds to breaking π bonds.

2.2. Computational Procedure for Determining the Hyperpolarizabilities. Several studies have demonstrated that the use of a split-valence or split-valence plus polarization basis set augmented with a set of *p* and *d* diffuse functions on the second-row atoms enables the reproduction of the second hyperpolarizability of large- and medium-size π-conjugated systems calculated with larger, and computationally less affordable, basis sets.[35,36] In the present study, the 6-31G*+*pd* basis set with *p* and *d* exponents of 0.0523 has been employed.[37] For the analysis of electron correlation effects on γ, a succession of methods has been adopted, starting with the UHF scheme. The *post*-

* Address correspondence to this author.
† Division of Chemical Engineering, Department of Materials Engineering Science, Graduate School of Engineering Science, Osaka University.
‡ Universitaires Notre-Dame de la Paix.
§ Department of Chemistry, Graduate School of Science, Osaka University.

10.1021/jp049637l CCC: $27.50
Published on Web 04/14/2004

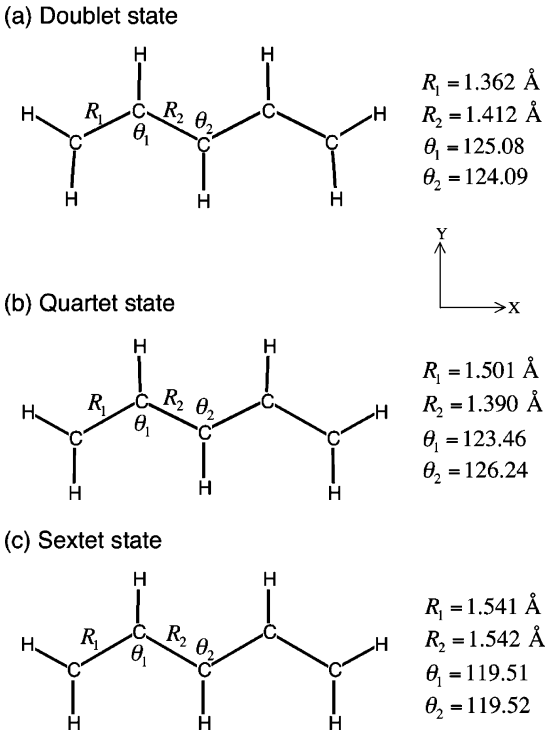

Figure 1. Structures of C_5H_7 radicals in (a) doublet, (b) quartet, and (c) sextet states. The structures are planar and belong to the C_{2v} point group.

UHF methods include the UHF−Møller−Plesset *n*th-order perturbation (UMP*n* ($n = 2-4$)), the UHF coupled cluster with single and double excitations (UCCSD), as well as with a perturbative treatment of the triple excitations, (UCCSD(T)), and the UHF-based quadratic configuration interaction scheme including all singles and doubles (UQCISD). In addition, the *l*-fold spin-projected UMP*n* methods with the Löwdin type spin projection,[38] i.e., PUHF ($l = 1$), PUMP2 ($l = 1$), and PUMP3 ($l = 1$), have also been applied to highlight the effects of spin contamination corrections on γ. Moreover, at the HF and MP2 levels, the corresponding restricted open-shell approaches (ROHF and ROMP2) have been employed while among the density functional theory (DFT) schemes, the hybrid B3LYP exchange-correlation functional has been adopted. All calculations have been performed with the Gaussian 98 program package.[39]

We confine our attention to the longitudinal components of γ. Although its vibrational counterpart would definitely deserve to be addressed in a forthcoming study, this study concentrates on the electronic contribution and more precisely on its static value. Indeed, for many of the theoretical approaches mentioned above, the methodologies and/or codes for evaluating their frequency-dependent analogues are nowadays not available. On the other hand, the static quantities can be obtained by adopting the finite field (FF) approach[40] that consists of evaluating the system energy for different amplitudes of the applied external electric field and, subsequently, in differentiating it numerically. To improve the accuracy on the γ values, a 4-point procedure (equivalent to a 7-point procedure for a nonsymmetric case) with field amplitudes of 0.0, 0.0010, 0.0020, and 0.0030 au[13] and/or the Romberg scheme[41] with field amplitudes of 0.0, 0.0010, 0.0020, and 0.0040 au were adopted. This has enabled us to reach an accuracy of 10−100 au on the static longitudinal second hyperpolarizability of the C_5H_7 radical. The power series expansion convention (*B* convention[42]) has been chosen for defining γ.

2.3. Second Hyperpolarizability Density Analysis. The second hyperpolarizability density analysis[7,13,34] has been used to characterize the spatial contributions of γ as well as of its α- and β-spin components. The contributions obtained from a pair of positive and negative (hyper)polarizability densities provide a description of local contributions of electrons to the total (hyper)polarizability. This method has also been extended to the vibrational components of (hyper)polarizabilities.[43] The static γ value can be expressed in atomic unit (au) by

$$\gamma = -\frac{1}{3!}\int r\rho^{(3)}(\boldsymbol{r})\, \mathrm{d}^3 r \tag{1}$$

where

$$\rho^{(3)}(\boldsymbol{r}) = \frac{\partial^3 \rho(\boldsymbol{r})}{\partial F\, \partial F\, \partial F}\Big|_{F=0} \tag{2}$$

This third-order derivative of the electron density with respect to the applied electric fields, $\rho^{(3)}(\boldsymbol{r})$, is referred to as the γ density. It is noted that the positive and negative values of γ densities multiplied by F^3 correspond respectively to the field-induced increase and decrease in the charge density (in proportion to F^3), which induce the third-order dipole moment (third-order polarization) in the direction from positive to negative γ densities. Therefore, the γ density map represents the relative phase and magnitude of change in the third-order charge densities between two spatial points with positive and negative values. The γ densities are calculated for a grid of points by using a numerical third-order differentiation of the electron densities (total, α and β) calculated by Gaussian 98. For treating the C_5H_7 radical, the origin is chosen to be the molecular center of mass, *XY* defines the molecular plane, and the longitudinal axis of the molecule is along the *X*-axis. The box dimensions ($-8 \le x \le 8$ Å, $-5 \le y \le 5$ Å, and $-5 \le z \le 5$ Å) ensure that the γ values obtained by integration are within 1−4% of the FF results. To explain the relationship between γ and $\rho^{(3)}(\boldsymbol{r})$, let us consider a pair of localized γ densities with positive and negative values. The sign of the γ contribution is positive when the direction from positive to negative γ density coincides with the positive direction of the coordinate system. The sign becomes negative in the opposite case. Moreover, the magnitude of the γ contribution associated with this pair of γ densities is proportional to the distance between them.

3. Results and Discussion

3.1. Electron Correlation Effect on γ of the Doublet State. Figure 2 and the second column of Table 1 show the impact of including electron correlation and of performing spin projection on the γ value of the C_5H_7 radical in the doublet state. In Figure 2, the methods **1**−**7** and **8**−**9** belong to the spin-unrestricted and spin-restricted schemes, respectively, while **10**−**12** belong to the spin-projected scheme. The methods are arranged in order of increasing correlation level in each scheme. The method **13** belongs to the DFT scheme. The second-order electron correlation correction is significant and positive: it enhances the γ value by more than 100% [151×10^2 au (UHF) and 304×10^2 au (UMP2)]. Although at the UMP3 (263×10^2 au) and UMP4SDQ (242×10^2 au) levels higher order electron correlation contributions are shown to correct the overshooting second-order contribution, the correction is not sufficient as compared to the UCCSD(T) value (215×10^2 au). From the comparison between the UMP4SDQ (242×10^2 au) and UMP4

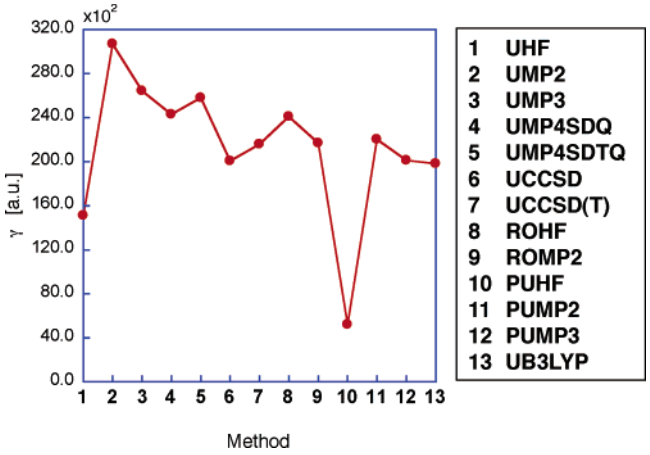

Figure 2. Electron-correlation dependency of γ [au] for the doublet C_5H_7 radical. The UHF, UMP2, UMP3, UMP4SDQ, UMP4SDTQ, UCCSD, UCCSD(T), PUHF, PUMP2, PUMP3, and UB3LYP results with 6-31G*+*pd* basis sets are shown.

TABLE 1: γ Values (in 100 au) for the Doublet, Quartet, and Sextet States of C_5H_7 Radical Obtained with Various Methods and the 6-31G*+pd Basis Set

	doublet	quartet	sextet
UHF	151	184	845
UMP2	304	366	1533
UMP3	263	315	1343
UMP4D	266	315	1356
UMP4DQ	253	300	1284
UMP4SDQ	242	297	1145
UMP4	258	328	1242
UCCSD	200	274	872
UCCSD(T)	215	300	931
UQCISD	193	272	696
ROHF	241	606	1106
ROMP2	217	−242	2354
PUHF	53	147	832
PUMP2	220	333	1539
PUMP3	201	295	1337
B3LYP	198	407	227

(258×10^2 au) values, the inclusion of the triple excitations in the fourth-order perturbation treatment brings a small positive contribution to γ. Actually, their inclusion at the CC level leads to a similar increase of γ [200×10^2 au (UCCSD) versus 215×10^2 au (UCCSD(T))].

On the other hand, correcting for spin contamination decreases the UHF, UMP2, and UMP3 γ values by 65%, 28%, and 24%, respectively [53×10^2 au (PUHF), 220×10^2 au (PUMP2), and 201×10^2 au (PUMP3)]. Similarly to the nonspin-projected case, the second-order Møller−Plesset correction substantially increases γ, whereas at the third-order level, this increase is slightly reduced. Strikingly, the low-order spin-projected PUMP2 value is close to the high-order correlated CCSD and CCSD(T) values. This suggests that, in the case of open-shell neutral systems in low spin states, obtaining a fast convergence of the γ value with respect to the order of electron correlation requires first the removal of spin contamination. The UQCISD (193×10^2 au) and UB3LYP (198×10^2 au) results are very similar to the best γ estimates. The restricted open-shell treatments provide γ values which are both in close agreement with the UCCSD(T) results [241×10^2 au (ROHF) and 217×10^2 au (ROMP2)], showing an improved convergence as a function of the inclusion of electron correlation with respect to the unrestricted and projected approaches.

TABLE 2: Expectation Value of S^2 for the Doublet, Quartet, and Sextet States of C_5H_7 Radical Obtained with Various Methods and the 6-31G*+pd Basis Set

	UHF	UMP2	PUHF	PUMP2	exact
doublet	1.171	1.056	0.684	0.728	0.750
quartet	3.911	3.847	3.746	3.750	3.750
sextet	8.815	8.770	8.749	8.750	8.750

Further insights into the spin contamination effects on the second hyperpolarizability of the doublet are provided by the expectation value of S^2 listed in Table 2 for HF and MP2 levels of approximations. In particular, at the UHF level the spin contamination is not negligible and it is overcorrected by using the PUHF ($l = 1$) scheme. The γ densities, as well as their α- and β-electron components, have been determined at the UHF, UQCISD, and UB3LYP levels and are shown in Figure 3. At the UHF level, the β-electron contribution (81×10^2 au) is larger than its α counterpart (76×10^2 au) though the doublet C_5H_7 possesses an excess of α π-electrons. In contrast, their relative contributions are inverted upon inclusion of electron correlation. Indeed, at the UQCISD level, the α-electron contribution is enhanced by 54% (117×10^2 au) whereas the β-electron contribution is slightly reduced (78×10^2 au). At the UHF and UQCISD levels, the main contributions to γ originate from the π-electron γ densities located at the molecule extremities and the amplitudes are the largest at the correlated level (Figure 3a,d). At the UHF level (see Figure 3b,c), the difference between the α- and β-electron contributions comes from the most-contributing end regions where the amplitudes of the β-electron γ densities are larger. The γ density delocalization is also observed for the β-electron contributions in the internal chain region. The larger β-electron γ densities are related to the presence of β-hole in a π-symmetry orbital. Indeed, due to the Pauli principle, the β π-electrons are predicted to fluctuate more significantly. This will be referred to as the Pauli effect and is responsible for the larger UHF γ densities of the β-electrons in both end regions.

The small reduction of the β-electron γ densities at the UQCISD level compared to the UHF case can be associated with the corresponding reduced spin polarization (Figure 4a,b). In addition, the β π-electron contribution increases in the middle region at the UQCISD level (Figure 3f) as compared to the UHF level (Figure 3c). This is related to the increase of delocalization of the β π-electrons in the middle region due to the correlation effects. As a result of these two antagonistic effects, the UQCISD β-electron contribution at the UQCISD level is only slightly smaller than its UHF analogue. On the other hand, the enhancement of α π-electron contribution upon including electron correlation is caused by an increase of delocalization that leads to the extension of the outer region of α π-electron distributions (see Figure 3e). Such extension of the outer region is predicted to be related to the fact that significant delocalization in the internal chain region is restricted by the Pauli principle while the α-spin density is important in the outer region (Figure 4b).

Therefore, correcting the overestimated UHF spin polarization leads to a small reduction of the β π-electron contributions whereas including electron correlation significantly increases the α π-electron contributions so that, at the UQCISD level, the γ contribution per π-electron is similar for the α- and β-electrons, whereas at the UHF level, the β component per π-electron is larger. These tendencies are substantiated by the γ reduction upon using spin-projected methods as well as by the enhancement of γ by the MP*n* methods. In addition, the

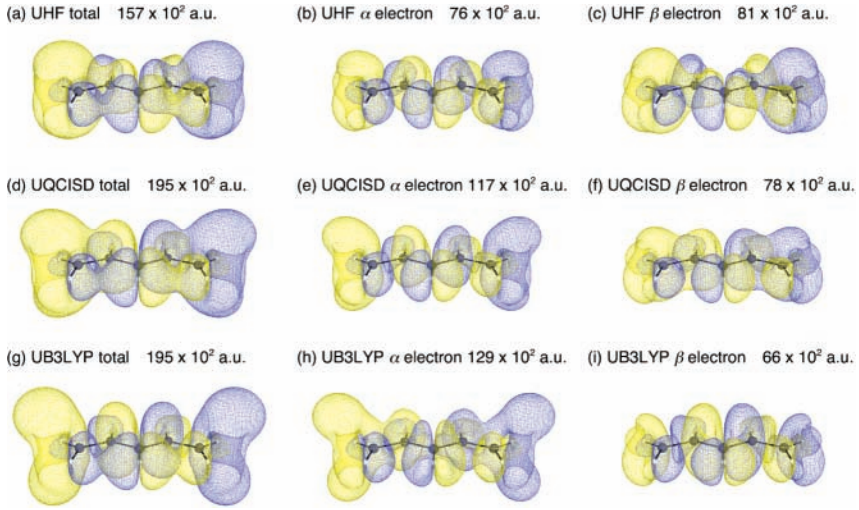

Figure 3. γ density distributions of the total, α- and β-electron contributions obtained at the UHF, UQCISD, and UB3LYP levels. The yellow and blue meshes represent positive and negative isosurfaces with ±20 au, respectively.

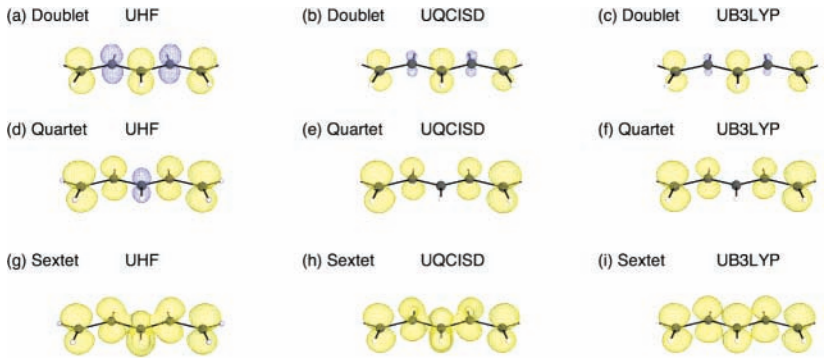

Figure 4. Spin density distributions for the doublet, quartet, and sextet states evaluated at the UHF, UQCISD, and UB3LYP levels. The yellow and blue meshes represent α- and β-spin densities with an isosurface with 0.02 au, respectively

UCC and UQCI calculations can involve both electron correlation and spin polarization corrections.

Finally, the applicability of the UB3LYP method to reproduce the γ of the doublet state is examined. The spin density at the UB3LYP level closely maps the UQCISD one (Figure 4b,c) while most of the γ contribution (66%) also comes from the α-electrons, which is a bit larger than at the UQCISD level (60%). Although the primary features of γ densities are similar at the UB3LYP and UQCISD levels, the UB3LYP α-electron γ density is slightly larger in the outer regions (Figure 3h), whereas for the β-electron contribution a decrease is observed at the extremities (Figure 3i).

3.2. Spin Multiplicity Effects on γ. The spin multiplicity effects on γ are investigated by comparing the doublet, quartet, and sextet states of the C_5H_7 radical (Table 1). At the exception of UB3LYP and ROMP2, all methods predict an enhancement of γ with the spin multiplicity, with a larger increase between the quartet and the sextet than between the doublet and the quartet. Similarly to the doublet state, the γ of the quartet is enhanced by almost a factor of 2 when adding second-order electron correlation corrections (UMP2: 366×10^2 au) to the UHF result (184×10^2 au) while higher order corrections at the UCCSD(T) level reduce this enhancement by 18% (300×10^2 au). Although the spin projection also reduces the UHF, UMP2, and UMP3 γ values of the quartet, the reduction is smaller than for the doublet and attains 20%, 9%, and 6%, respectively. Again, the PUMP2 and PUMP3 values are good approximations to the UCCSD(T) results. This decrease of the spin projection effect with the spin multiplicity is related to the reduction of spin polarization (Figure 4) and spin contamination (Table 2) as a result of a larger number of α π-electrons. On the contrary, the ROHF and ROMP2 values are much different, between themselves as well as with respect to the UCCSD(T) γ value. These poor results are attributed to the missing electron correlation effects.

For the sextet state, the UHF value (845×10^2 au) is similar to the best UCCSD(T) result (931×10^2 au), whereas the MP*n* values are strongly overestimated. Contrary to the case of the quartet, the spin projection effect is shown to be negligible as expected (Table 2). Moreover, higher order electron correlation effects at the UCCSD and UCCSD(T) levels are necessary for correcting the overshot UMP*n* and PUMP*n* values. The ROHF and ROMP2 values are larger than their unrestricted (and projected) analogues showing again the impact of the missing electron correlation effects.

Although the UB3LYP method reproduces the UCCSD(T) γ value of the doublet state, it overshoots the γ of the quartet state by 36% while it significantly undershoots (by 76%) the sextet γ value. For the quartet, the deficiency of the UB3LYP method seems to originate in the self-interaction error associated with the large CC bond lengths. Indeed, it was pointed out by Mori-Sánchez et al.[44] that approximate exchange-correlation functionals incorrectly describe the polarizability of weakly interacting molecules with a fractional charge.[44] The alternation between large γ underestimation and large γ overestimation for different spin state, which is obtained when using DFT schemes with usual exchange-correlation functionals, reminded the authors of increasingly large oligomers and push−pull com-

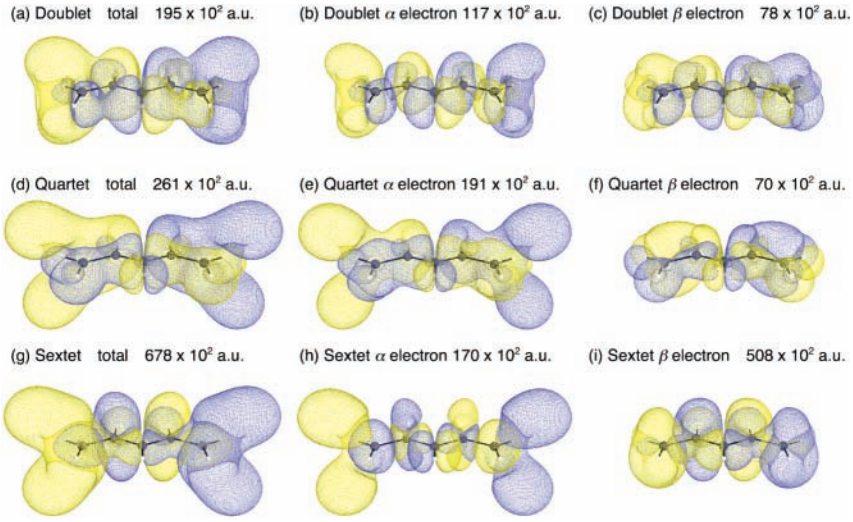

Figure 5. γ density distributions for the total, α- and β-electron contributions of the doublet, quartet, and sextet states determined at the UQCISD level. The yellow and blue meshes represent positive and negative γ densities with isosurfaces with ±20 au for doublet and quartet states and ±40 au for sextet state.

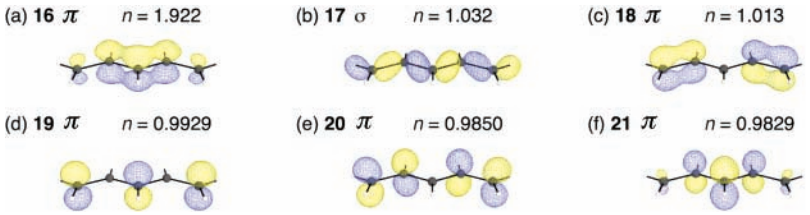

Figure 6. Natural orbitals and their occupation numbers for the highest **16**−**21** in sextet state at the UQCISD level. The yellow and blue meshes represent positive and negative isosurfaces with ±0.08 au, respectively.

pounds where the drawbacks of the exchange-correlation functional have been related to their shortsightedness.[45−47] Although more investigation is required, the origin of these failures could be the same.

Figure 5 compares the UQCISD total, α- and β-electron γ densities of the three spin states. In the quartet state (Figure 5d−f), the total γ density contribution is composed of two large and delocalized positive π-electron distributions as well as of two smaller delocalized negative σ-electron distributions. With respect to the doublet (Figure 5a−c), these distributions are enhanced at the level of the end CC bonds due to the β-electron contribution (70×10^2 au), as well as in the outer region due to the remarkable extension of the α-electron γ density (191×10^2 au). However, when normalizing the contributions to the number of α or β π-electrons, the relative β contribution increases substantially when going from the doublet (39×10^2 au per β π-electron) to the quartet (70×10^2 au per β π-electron), whereas for the α contribution the increase is smaller: from 39×10^2 au per α π-electron in the doublet to 48×10^2 au in the quartet. Such effective enhancements of the α- and β-electron contributions and their delocalized distributions in the quartet state can be explained by considering the intermediate π bond breaking nature of the outer CC bonds (R_1 = 1.501 Å) of the quartet state, which is associated with larger γ values.[32]

In contrast to the quartet state, in the sextet state (Figure 5g−i, Table 1), the β-electron contribution is so large (508×10^2 au) that it dominates γ (75%) and enhances the total γ value by 255% and 360% with respect to the quartet and doublet states, respectively. The α-electron contribution (170×10^2 au) is 11% smaller (45% larger) than in the quartet (doublet) state. When normalizing the contributions to the number of α π-electrons, the sextet γ value—obtained by considering 5 contributing π-electrons—is smaller than both the doublet (13%) and quartet (28%) values. This reduction of the sextet α-electron contribution follows the behavior of the second hyperpolarizability in the H_2 molecule upon elongating the bond length:[32,33] γ increases when stretching the bond from equilibrium (weak correlation regime) to intermediate correlation regime and then decreases when the bond length gets larger (strong correlation regime). Of course, the analogy is not complete because in the C_5H_7 radical case the CC bonds are similar to single bonds and the unpaired electrons and sites are not identical as in H_2. Actually, the α π-electron γ density (Figure 5h) is particularly extended in the outer region as for the quartet (Figure 5e) and contributes positively to γ. A small localized π-electron feature with negative contributions is located in the internal chain region and could originate in the strong correlation among the 5 α π-electrons (one on each C site) due to the Pauli principle. Moreover, σ-electrons bring an additional negative contribution in such a way that the α-electron contribution slightly decreases when going from the quartet to the sextet.

In contrast, as seen from Figure 5i, the β-electron contribution is larger and positive for the σ-electrons while being smaller and negative for the π-electron. To elucidate the different hyperpolarization effects in the sextet state, we investigated at the UQCISD level the natural orbitals. Together with their occupation numbers they are displayed in Figure 6. It is found that in the sextet state the order of the lowest π-orbital **16** and the highest σ-orbital **17** is inverted with respect to the doublet and quartet states in such a way that an unpaired α-electron lies in the σ-orbital **17** instead of the π-orbital **16**, which is doubly occupied. This feature is understood by the fact that the σ-orbital **17** is composed of localized CC σ-bond distributions with mutually opposite phase while the π-orbital **16** has a delocalized distribution over the entire chain region. As a result,

there are six π-electrons (five α and one β), as well as one α-electron, and a β-hole in a σ-orbital. This feature supports the spin distribution of the sextet state at the UHF and UQCISD levels, which presents a partial σ-symmetry character as shown in Figure 4g,h. The presence of a β-hole in the σ-symmetry orbital **17** enables large field-dependent fluctuations of the β-electron density and accounts for the substantial β-electron contribution to γ. On the other hand, the fluctuations of the β-electron in the doubly occupied π-orbital **16** are small because of the stable bonding nature of the orbital. The γ contribution of this π-electron of spin β, which is shown in the middle three C sites region, is negative as for those systems where low-energy virtual excitation processes (type II) dominate the response.[7,13] In analogy to refs 31 and 32, the α electrons belong to the strong correlation regime due to the Pauli effects between the five electrons of the same spin while the β-electrons belong to the intermediate correlation regime. At the UB3LYP level, the σ-orbital of highest energy is below the five singly occupied π-orbitals so that there is no β-hole in the σ-symmetry orbital. This is confirmed by the UB3LYP spin density of the sextet (Figure 4i). The strong γ underestimation is therefore explained by the remarkable decrease of the β-electron contribution (314 au) due to the nonexistence of β σ-hole and β π-electrons and the smaller α-electron contribution (223×10^2 au) than that (337×10^2 au) in the quartet state at the UB3LYP level, the feature of which is associated with the strong correlation regime for the α π-electrons in the sextet state at the UB3LYP level.

4. Concluding Remarks

The spin multiplicity effects on the second hyperpolarizability have been investigated for a small-size open-shell neutral conjugated model, the C_5H_7 radical, in the doublet, quartet, and sextet states. It turns out that the second hyperpolarizability increases with the spin multiplicity, with a larger difference between the quartet and the sextet than between the doublet and the quartet. The increase from the doublet to the quartet is mostly attributed to the enhanced contribution from the outer α π-electron densities that result from the Pauli effect. On the other hand, the substantial γ value of the sextet originates from the presence of a β-hole in a σ-symmetry orbital. These variations in γ value have been related to the degree of bond breaking and the electron correlation regime.[31,32] In particular, the intermediate correlation regime (quartet and β-electrons of the sextet) is associated with the largest γ value whereas for the weak (doublet) and strong (α-electrons of the sextet) correlation regimes, the third-order NLO responses are smaller.

For such systems, highly correlated methods (UCCSD, UCCSD(T), and UQCISD) turn out to be necessary for a qualitative and (semi)quantitative study. Nevertheless, for the lower spin states, the spin-projected low-order UMP*n* methods, e.g., PUMP2, and low-order restricted open-shell MP*n* treatment, e.g., ROMP2, nicely reproduce the UCCSD(T) results. In contrast, the UB3LYP method fails in determining both quantitative and qualitative effects of the spin multiplicity on γ.

Due to the large enhancement of γ with spin multiplicity, neutral open-shell conjugated systems appear therefore as candidates for a new class of NLO systems, "spin-enhanced NLO systems". In addition, one can also speculate the possibility of controlling γ by (externally) modulating the spin multiplicity. Actually, lots of spin-controlling schemes have been proposed in the field of molecular magnetism for open-shell compounds.[48] Subsequently, these results also suggest the interest for studying the NLO properties of such molecular magnetic systems. However, since such systems involve changes of not only the spin multiplicity but also the charge, the investigation of the NLO properties of open-shell charged systems is now in progress.

Acknowledgment. This work was supported by Grant-in-Aid for Scientific Research (No. 14340184) from the Japan Society for the Promotion of Science (JSPS). E.B. thanks the Interuniversity Attraction Pole on "Supramolecular Chemistry and Supramolecular Catalysis" (IUAP No. P5-03) for her postdoctoral grant while B.C. thanks the Belgian National Fund for Scientific Research for his Senior Research Associate position. Some of the calculations were performed on the Pentium III/Pentium IV cluster of the CTA lab as well as on the SUN V880 computers of the ISCF center for which the authors acknowledge the financial support of the FNRS.

References and Notes

(1) Williams, D. J., Ed. *Nonlinear Optical Properties of Organic and Polymeric Materials*; ACS Symp. Ser. 233; American Chemical Society: Washington, DC, 1984.

(2) Chemla, D. S.; Zyss, J., Eds. *Nonlinear optical properties of organic molecules and crystals*; Academic Press: New York, 1987; Vols. 1 and 2.

(3) Prasad, N. P.; Williams, D. J. *Introduction to Nonlinear Optical Effects in Molecules and Polymers*; Wiley: New York, 1991.

(4) Michl, J., Ed. Optical Nonlinearities in Chemistry. *Chem. Rev.* **1994**, *94*.

(5) Karna, S. P.; Yeates, A. T., Eds. *Nonlinear Optical Materials. Theory and Modeling*; ACS Symp. Ser. 628; American Chemical Society: Washington, DC, 1996.

(6) Bosshard, Ch.; Sutter, K.; Prêtre, Ph.; Hulliger, J.; Flosheimer, M.; Kaatz, P.; Günter, P. *Organic Nonlinear Optical Materials*; Gordon and Breach: Basel, Switzerland, 1995.

(7) Nakano, M.; Yamaguchi, K. In *Trends in Chemical Physics*; Research Trends: Trivandrum, India, 1997; Vol. 5, pp 87−237,

(8) Nalwa, H. S., Ed. *Handbook of Advanced Electronic and Photonic Materials and Devices*; Vol. 9, Nonlinear Optical Materials; Academic Press: New York, 2001.

(9) Nakano, M.; Yamaguchi, K. Mechanism of Nonlinear Optical Phenomena for π-Conjugated Systems. In *Organometalic Conjugation*; Nakamura, A., Ueyama, N., Yamaguchi, K., Eds.; Koudansha-Springer: New York, 2002.

(10) Nakano, M.; Yamaguchi, K. In *Advances in Multi-Photon Processes and Spectroscopy*; World Scientific: Singapore, 2003; Vol. 15, pp 1−146.

(11) de Melo, C. P.; Silbey, R. *Chem. Phys. Lett.* **1987**, *140*, 537.

(12) Nakano, M.; Yamaguchi, K. *Chem. Phys. Lett.* **1993**, *206*, 285.

(13) Nakano, M.; Shigemoto, I.; Yamada, S.; Yamaguchi, K. *J. Chem. Phys.* **1995**, *103*, 4175.

(14) Nakano, M.; Kiribayashi, S.; Yamada, S.; Shigemoto, I.; Yamaguchi, K. *Chem. Phys. Lett.* **1996**, *262*, 66.

(15) (a) de Melo, C. P.; Fonseca, T. L. *Synth. Met.* **1997**, *85*, 1085. (b) de Melo, C. P.; Fonseca, T. L. *Chem. Phys. Lett.* **1996**, *261*, 28.

(16) Kirtman, B.; Champagne, B. *Int. Rev. Phys. Chem.* **1997**, *16*, 389.

(17) Yamada, S.; Nakano, M.; Shigemoto, I.; Kiribayashi, S.; Yamaguchi, K. *Chem. Phys. Lett.* **1997**, *267*, 438.

(18) Champagne, B.; Deumens, E.; Öhrn, Y. *J. Chem. Phys.* **1997**, *107*, 5433.

(19) An, Z.; Wong, K. Y. *J. Chem. Phys.* **2001**, *114*, 1010.

(20) Champagne, B.; Kirtman, B. in ref 8, Chapter 2, p 63.

(21) Nakano, M.; Fujita, H.; Takahata, M.; Yamaguchi, K. *J. Am. Chem. Soc.* **2002**, *124*, 9648.

(22) Fujita, H.; Nakano, M.; Takahata, M.; Yamaguchi, K. *Chem. Phys. Lett.* **2002**, *358*, 435.

(23) Champagne, B.; Spassova, M.; Jadin, J. B.; Kirtman, B. *J. Chem. Phys.* **2002**, *116*, 3935.

(24) Di Bella, S.; Fragalà, I.; Ledoux, I.; Marks, T. J. *J. Am. Chem. Soc.* **1995**, *117*, 9481.

(25) Karna, P. S. *J. Chem. Phys.* **1996**, *104*, 6590; erratum **1996**, *105*, 6091.

(26) Nakano, M.; Yamada, S.; Yamaguchi, K. *Bull. Chem. Soc. Jpn.* **1998**, *71*, 845.

(27) Yamada, S.; Nakano, M.; Yamaguchi, K. *J. Phys. Chem. A* **1999**, *103*, 7105.

(28) Nakano, M.; Yamada, S.; Yamaguchi, K. *Chem. Phys. Lett.* **1999**, *311*, 221.

(29) Champagne, B.; Kirtman, B. *Chem. Phys.* **1999**, *245*, 213.

(30) Yamada, S.; Nakano, M.; Yamaguchi, K. *Int. J. Quantum Chem.* **1999**, *71*, 329.

(31) Yamanaka, S.; Okumura, M.; Nakano, M.; Yamaguchi, K. *J. Mol. Struct.* **1994**, *310*, 205.

(32) Nakano, M.; Nagao, H.; Yamaguchi, K. *Phys. Rev. A* **1997**, *55*, 1503.

(33) Nakano, M.; Yamada S.; Yamaguchi, K. *JCMSE*. In press.

(34) Nakano, M.; Yamaguchi, K.; Fueno, T. *Chem. Phys. Lett*. **1991**, *185*, 550.

(35) Hurst, G. J. B.; Dupuis, M.; Clementi, E. *J. Chem. Phys.* **1988**, *89*, 385.

(36) Champagne, B.; Kirtman, B. in ref 8, Chapter 2, p 63.

(37) The 6-31G*+pd basis set turns out to be a good compromise between computational efficiency and property accuracy from UHF, UMP2, and PUMP2 calculations carried out with several basis sets. The latter include basis sets derived from the 6-31G*+*pd*, i.e. 6-31G*, 6-31G*+*d*, and 6-31G*+*p*, the Dunning−Huzinaga triple-ζ basis set [Huzinaga, S. *J. Chem. Phys.* **1965**, *42*, 1293. Dunning, T. H. *J. Chem. Phys.* **1971**, *55*, 716] augmented with diffuse functions as well as the cc-pvdz, cc-pvtz, and aug-cc-pvdz basis sets. The diffuse functions added to the Dunning−Huzinaga triple-ζ basis set have been taken from the electrical property (ELP) basis set of Liu and Dykstra [Liu, S. Y.; Dykstra, C. E. *J. Phys. Chem.* **1987**, *91*, 1749] that has been designed for hyperpolarizability calculations. TZ + ELP(s) means that one set of *s* diffuse functions has been added to C and H atoms, TZ + ELP(sp) = TZ + ELP(s) plus two sets of *p* diffuse functions on H and C atoms while TZ + ELP(spd) = TZ + ELP(sp) + three sets of *d* functions on the C atoms. By using the 6-31G* (89), 6-31G*+*d* (119), 6-31G*+*p* (104), 6-31G*+*pd* (134), TZ (91), TZ+ELP(s) (103), TZ+ELP(sp) (175), TZ+ELP(spd) (265), cc-pvdz (110), cc-pvtz (280), and aug-cc-pvdz (188) basis sets where the numbers in parentheses correspond to the number of basis functions for treating C_5H_7, γ amounts (in 10^2 au) to 96, 125, 139, 151, 115, 119, 136, 145, 83, 94, and 109 at the UHF level, to 167, 227, 259, 304, 212, 221, 294, 298, 239, 284, and 345 at the UMP2 level, and to 122, 171, 189, 220, 153, 160, 202, 216, 145, 175, and 213 at the PUMP2 level, respectively. Thus, the 6-31G*+*pd* basis set provides γ values which are in close agreement with those evaluated with the much larger TZ+ELP(spd) and aug-cc-pvdz basis sets, especially at correlated levels.

(38) Löwdin, P. O. *Phys. Rev.* **1955**, *97*, 1509.

(39) Frisch, M. J.; Trucks, G. W.; Schlegel, H. B.; Scuseria, G. E.; Robb, M. A.; Cheeseman, J. R.; Zakrzewski, V. G.; Montgomery, J. A.; Stratmann, R. E.; Burant, J. C.; Dapprich, S.; Millam, J. M.; Daniels, A. D.; Kudin, K. N.; Strain, M. C.; Farkas, O.; Tomasi, J.; Barone, V.; Cossi, M.; Cammi, R.; Mennucci, B.; Pomelli, C.; Adamo, C.; Clifford, S.; Ochterski, J.; Petersson, G. A.;. Ayala, P. Y.; Cui, Q.; Morokuma, K.; Malick, D. K.; Rabuck, A. D.; Raghavachari, K.; Foresman, J. B.; Cioslowski, J.; Ortiz, J. V.; Stefanov, B. B.; Liu, G.; Liashenko, A.; Piskorz, P.; Komaromi, I.; Gomperts, R.; Martin, R. L.; Fox, D. J.; Keith, T.; Al-Laham, M. A.; Peng, C. Y.; Nanayakkara, A.; Gonzalez, C.; Challacombe, M.; Gill, P. M. W.; Johnson, B. G.; Chen, W.; Wong, M. W.; Andres, J. L.; Head-Gordon, M.; Replogle, E. S.; Pople, J. A. *Gaussian 98*, revision A.1; Gaussian, Inc.; Pittsburgh, PA, 1998.

(40) Cohen, H. D.; Roothaan, C. C. J. *J. Chem. Phys.* **1965**, *43*, S34.

(41) Jacquemin, D.; Champagne, B.; André, J. M. *Int. J. Quantum Chem.* **1997**, *68*, 679.

(42) Willetts, A.; Rice, J. E.; Burland, D. M.; Shelton, D. P. *J. Chem. Phys.* **1992**, *97*, 7590.

(43) Bishop, D. M.; Bouferguene, A. *Int. J. Quantum Chem.* **2000**, *78*, 348.

(44) Mori-Sánchez, P.; Wu, Q.; Yang, W. *J. Chem. Phys.* **2003**, *119*, 11001.

(45) Champagne, B.; Perpète, E. A.; van Gisbergen, S. J. A.; Snijders, J. G.; Baerends, E. J.; Soubra-Ghaoui, C.; Robins, K. A.; Kirtman, B. *J. Chem. Phys.* **1999**, *109*, 10489; *erratum* **1999**, *110*, 11664.

(46) van Gisbergen, S. J. A.; Schipper, P. R. T.; Gritsenko, O. V.; Baerends, E. J.; Snijders, J. G.; Champagne, B.; Kirtman, B. *Phys. Rev. Lett.* **1999**, *83*, 694.

(47) Champagne, B.; Perpète, E. A.; Jacquemin, D.; van Gisbergen, S. J. A.; Baerends, E. J.; Soubra-Ghaoui, C.; Robins, K. A.; Kirtman, B. *J. Phys. Chem. A* **2000**, *104*, 4755.

(48) Yamaguchi, K.; Kawakami, T.; Yamaki, D.; Yoshioka, Y. Theory of Molecular Magnetism. In *Molecular Magnetism*; Ito, K., Kinoshita, M., Eds.; Kodansha, and Gordon and Breach: New York, 2000; pp 9−48.